Determination of cirrus cloud optical properties using ground-based Atmospheric Emitted Radiance Interferometer and Raman lidar measurements

Final Report

PI: Daniel H. DeSlover

Grant Number: NNG04GB01G
(Effective Date 1 December 2003
through 30 November 2004)

University of Wisconsin-Madison
Space Science and Engineering Center
1225 W. Dayton St.
Madison, WI 53706

Table of Contents

1.0 Introduction

This report comprises the "Contract Final Report", Unsolicited Grant NNG04GB01G from NASA Goddard Space Flight Center to the University of Wisconsin Space Science and Engineering Center (UW-SSEC). This report describes the activities performed for the time period comprising 1 December 2003 through 30 November 2004.

2.0 Summary by Task

The single task proposed under the NASA contract is summarized in the following sections organized by case study date. The identification of each case study, and the corresponding section in which they appear in this report, is given below:

Case Study	Description	Report Section
Case 1	AFWEX 2000, 8 December 2000	Section 2.1
Case 2	AFWEX 2000, 7 December 2000	Section 2.2
Case 3	Texas 2002, 29 November 2002	Section 2.3

Table 1: Case study analsys, description, and report Section number.

2.1 AFWEX 2000 Case Study, 8 December 2000

The Atmospheric Radiation Measurement First ISSCP Regional Experiment (ARM-FIRE) Water Vapor Experiment (AFWEX) was conducted during November-December 2000 at the Southern Great Plains (SGP) Climate Research Facility (CRF). The primary AFWEX field campaign goals were to characterize the accuracy of current water vapor measurements in the upper troposphere and to develop techniques for improving water vapor measurements under a wide range of conditions (e.g., clear, cloudy). A cirrus case, which occurred on 8 December 2000, was sampled using high spectral resolution infrared measurements from above (NPOESS Airborne Sounder Testbed-Interferometer; NAST-I) on the Proteus aircraft and below (Atmospheric Emitted Radiance Interferometer; AERI). Results will be compared for 4 aircraft overpasses (flight track shown on right) of the ground-based AERI.

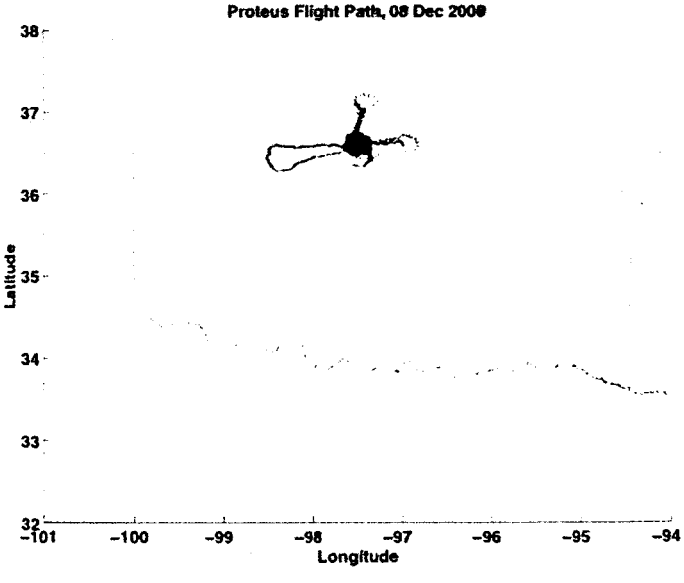

The general approach to the cloud optical depth (OD) retrieval utilizes an average cloud base and cloud top altitude, derived from lidar data, during the AERI scene dwell time. Radiosondes are released several times during the day, which provide atmospheric state information required to calculate the clear sky radiance contribution and atmospheric transmissivity between the surface and cloud base. An atmospheric transmission profile is determined for each radiosonde profile. Atmospheric temperature and transmissivity are then interpolated for each AERI scene observation to invert the cloud

absorption OD. NAST-I measurements were limited to an aircraft location that was within a box defined by +/- 0.1 degrees latitude/longitude of the AERI surface instrument location. This approach was also used because an airborne lidar was not available. Therefore, the cloud boundaries for the aircraft-based cloud retrievals were also determined by the ground-based lidar measurements; which included the CRF Raman Lidar (CARL) and NASA GSFC Scanning Raman Lidar (SRL).

Figure 2 shows CARL cloud boundaries (upper panel), determined from the lidar depolarization ratio, between 0000 and 1000 UTC on 8 Dec 2000. Aircraft measurements occurred between 0100 and 0300 UTC. Optical depth results from NAST-I (circles), AERI (thin lines), CARL (heavy black line), and SRL (heavy green line) are presented in the second panel. The CARL and AERI, which operated during the entire period, demonstrate very good correlation despite differences in instrument field-of-view and observation dwell times. Good agreement is also seen in the SRL data, which operated during the aircraft overpass times. The red circles represent NAST-I aircraft measurements, where all nadir and 7.5 degree scan angle results were averaged for each overpass; intended to best represent a single AERI measurement. Aircraft measurements were consistent with the ground-based results. The third and fourth panels provide bulk cloud effective radius and number density, respectively, for both hexagonal column (asterisks) and spherical (blue circles) ice crystals. Aircraft data are again shown for comparison (red circles) for each of the four ground site overpasses.

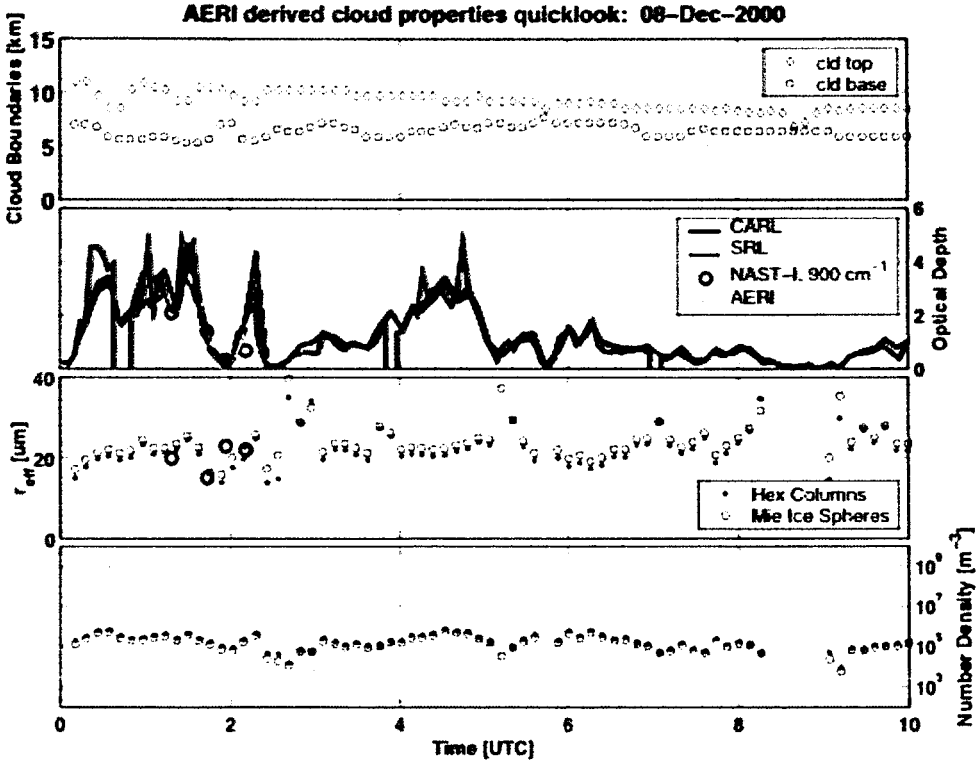

Figure 2. Time series of cloud optical properties on 8 Dec 2000, from 0000 through 1000 UTC. Top panel indicates lidar measured cloud top and cloud base use in the analysis. Second panel gives cloud optical depth measured from the ground-based lidars (CARL and SRL), ground-based AERI, and aircraft-based NAST-I. The third and fourth panels show bulk cloud effective radius and associated number density, respectively. Ice crystal were assumed to be hexagonal column (asterisks) or spheres (circles).

2.2 AFWEX 2000, 7 December 2000

Similar to Section 2.1, but no ancillary aircraft or SRL measurements. This case provides an example of thin cirrus measurements with error analysis for the Raman lidar (black dots) and AERI (blue circles) on 7 December 2000 between 1700 and 2400 UTC. It also represents the early stages of cirrus development (the event which continued, and is analyzed, in Section 2.1). The upper panel shows cirrus cloud OD from 1700 through 2400 UTC derived from both AERI and CARL data; where the OD are generally small (< 1), yet exhibit good agreement for all values. The primary purpose for analyzing a thin cirrus case was to demonstrate the increased uncertainty in retrieving ice particle bulk effective radii (bottom panel). The emitted radiance from the thin cloud is dominated by gaseous emission, mostly water vapor; hence the large variance in size retrieval relative to similar data shown in Fig. 2. A mean effective radius of about 22 μm is similar to values early the next day (Fig. 2). As the cloud OD increases above 0.5 (e.g., early the next day) the variability decreases as the value converges to 22 μm.

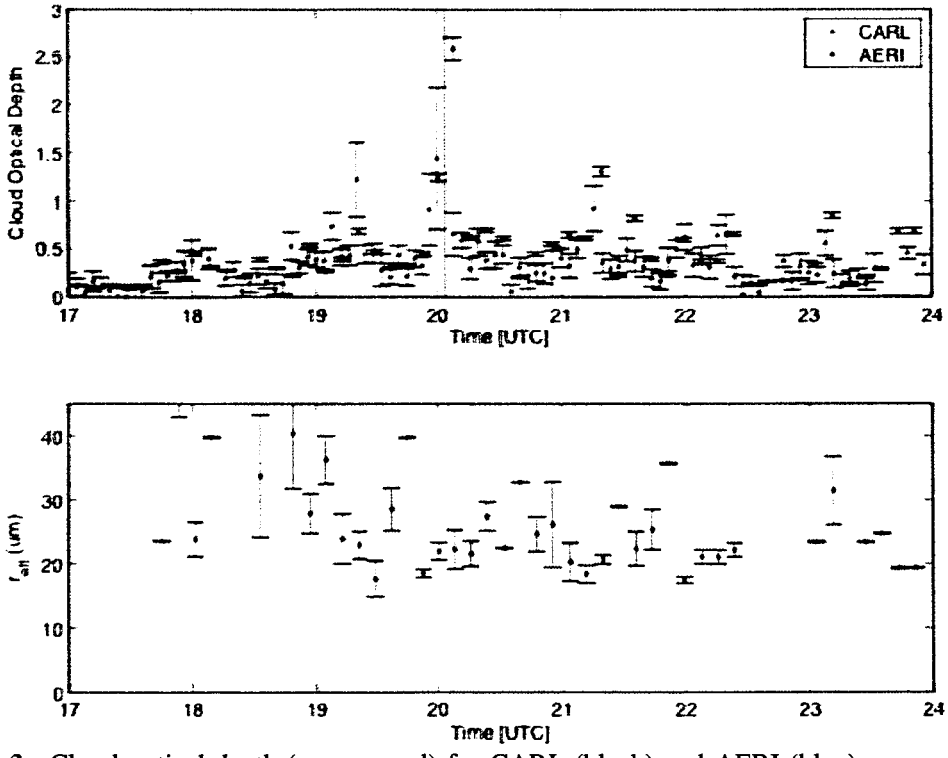

Figure 3. Cloud optical depth (upper panel) for CARL (black) and AERI (blue) measurements acquired between 1700 and 2400 UTC on 7 December 2000. Results indicate good agreement in derived cloud OD for optically thin (< 0.5) cirrus, but increased noise in AERI size retrieval (bottom panel) due to gaseous (e.g., water vapor) emission dominating the downwelling column radiance.

2.3 Texas 2002, 29 November 2002

A few changes were made to the AERI instrument in 2002, which demonstrated the ability to acquire emission spectra in rapid-sample mode. This increased the instrument sample rate from one measurement per seven-minute nominal time to sub-minute intervals. Figure 4 shows results for a 29 November 2002 cirrus case (Texas 2002 field campaign). The top panel gives lidar measured cloud boundaries as a function of time (shown from 0400 to 1100 UTC). The cirrus are seen to be of a single layer then becoming tenuous after 0700 UTC. The middle panel shows the cloud OD from both the CARL (solid black line) and AERI (blue) for the entire time period. One feature of particular interest occurs between

0800 and 1000 UTC, where it appears a wave cloud has advected over the site. A significant oscillation in OD, ranging between 0 and 2, over this duration is readily apparent in both the CARL and AERI data. This is a striking feature, and a notable improvement in the AERI measurement capability due to rapid-sample operation. Note that the CARL data are two-minute averages, which gently smooth the oscillation feature slightly. The bottom panel shows the cloud particle bulk effective radius. The effective size results are consistent with the thin cirrus data from Section 2.2, where the retrieved size capability improves for cloud OD > 0.5 (i.e., 0500 through 0700 UTC).

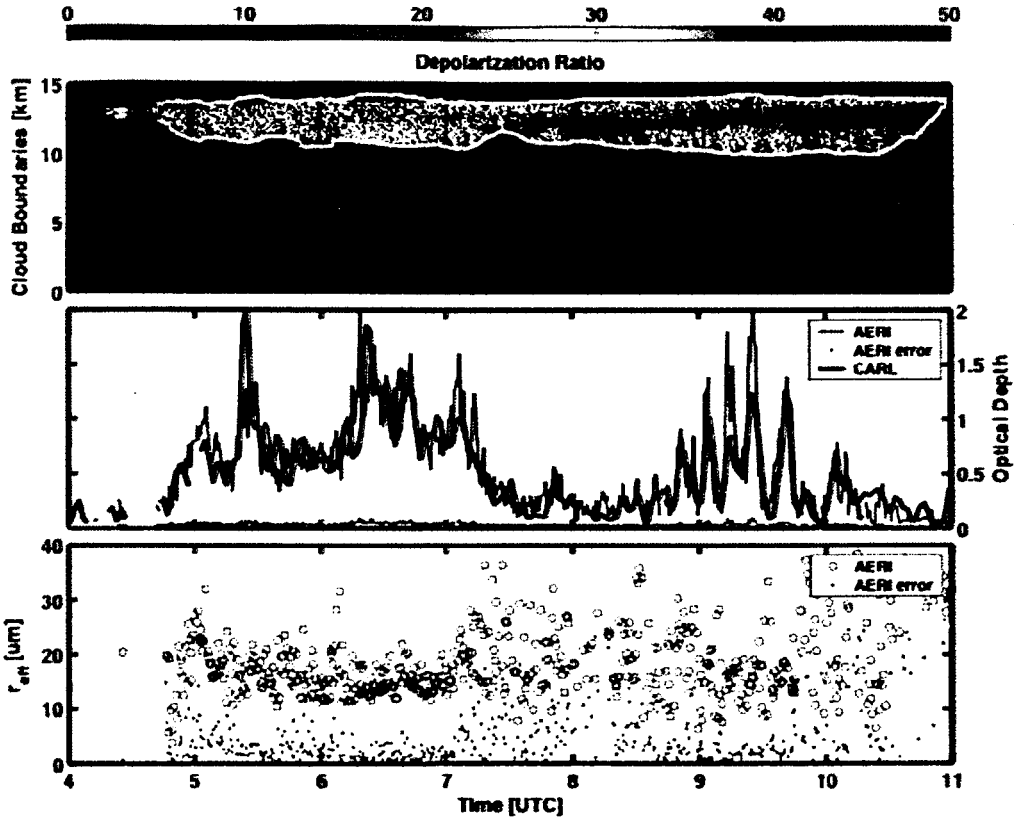

Figure 4. Retrieved cloud optical properties for 29 November 2002 (Texas 2002) cirrus case. The AERI was operating in rapid-sample mode (sub-minute dwell times), which afforded the opportunity to analyze a wave cloud (0800 through 1000 UTC). Top panel shows lidar depolarization and cloud boundaries used in the AERI retrieval. Middle panel shows CARL and AERI measured cloud optical depth, where the two-minute averaged CARL data wash out the features measured by the AERI. Bottom panel shows cloud effective radius.

3.0 Conclusions

This section contains statements summarizing any significant results, lessons learned, and suggestions for future activities.

- The Raman lidar and AERI cloud optical depths agree well (within 5 percent) over a range of cloud optical depths (0 to 3; where the lidar measurement capability is the limiting factor). Implementation of a rapid-sample mode to the AERI software (increase in sample frequency from 7 minute to sub-minute sample rate) has improved the ability to study cloud structure features.
- Particle size retrieval is dependent upon the cloud optical depth. As seen in case 2 (Section 2.1), the variability in size increases for smaller cloud optical depth. As the cloud OD increases (Case 1, Section 2.1) the retrieved size approaches a more uniform value. This would be expected as the gaseous emission portion of the downwelling radiance dominates the measurement for optically thin clouds. As the cloud OD increases, the emission signal also increases, such that uncertainties due to gaseous atmospheric emission are suppressed; where the lower limit appears to be near 0.75. Results from above and below the cloud (Case 1, Section 2.1) were consistent.
- Future studies with additional ice crystal habits would be useful to gauge the effect of ice crystal habit on the infrared radiance spectrum. The application of Raman lidar derived particle size could also be compared to the AERI measurements. Also, the current approach assumes uniform emission from the cloud layer. The algorithm could be modified to use the Raman lidar optical depth profile to effectively weight the cloud emission.